

Supplementary material

Inhibition of IL-12/IL-23 signaling reduces Alzheimer's disease-like pathology and cognitive decline

Johannes vom Berg^{1,6}, Stefan Prokop^{2,6}, Kelly R. Miller², Juliane Obst², Roland E. Kälin², Ileana Lopategui-Cabezas^{2,5}, Anja Wegner², Florian Mair¹, Carola G. Schipke^{2,3}, Oliver Peters³, York Winter⁴, Burkhard Becher^{1,7} and Frank L. Heppner^{2,7}

¹Institute of Experimental Immunology, University of Zurich, 8057 Zürich, Switzerland

²Department of Neuropathology, Charité – Universitätsmedizin Berlin, 10117 Berlin, Germany

³Department of Psychiatry, Charité – Universitätsmedizin Berlin, Campus Benjamin Franklin, 10117 Berlin, Germany

⁴Cognitive Neurobiology and Berlin Mouse Clinic for Neurology and Psychiatry, Humboldt University, Dorotheenstraße 94, 10117 Berlin, Germany

⁵present address: Institute of Basic and Preclinical Sciences “Victoria de Girón”, Medical University of Havana, Cuba

⁶These authors contributed equally to this work

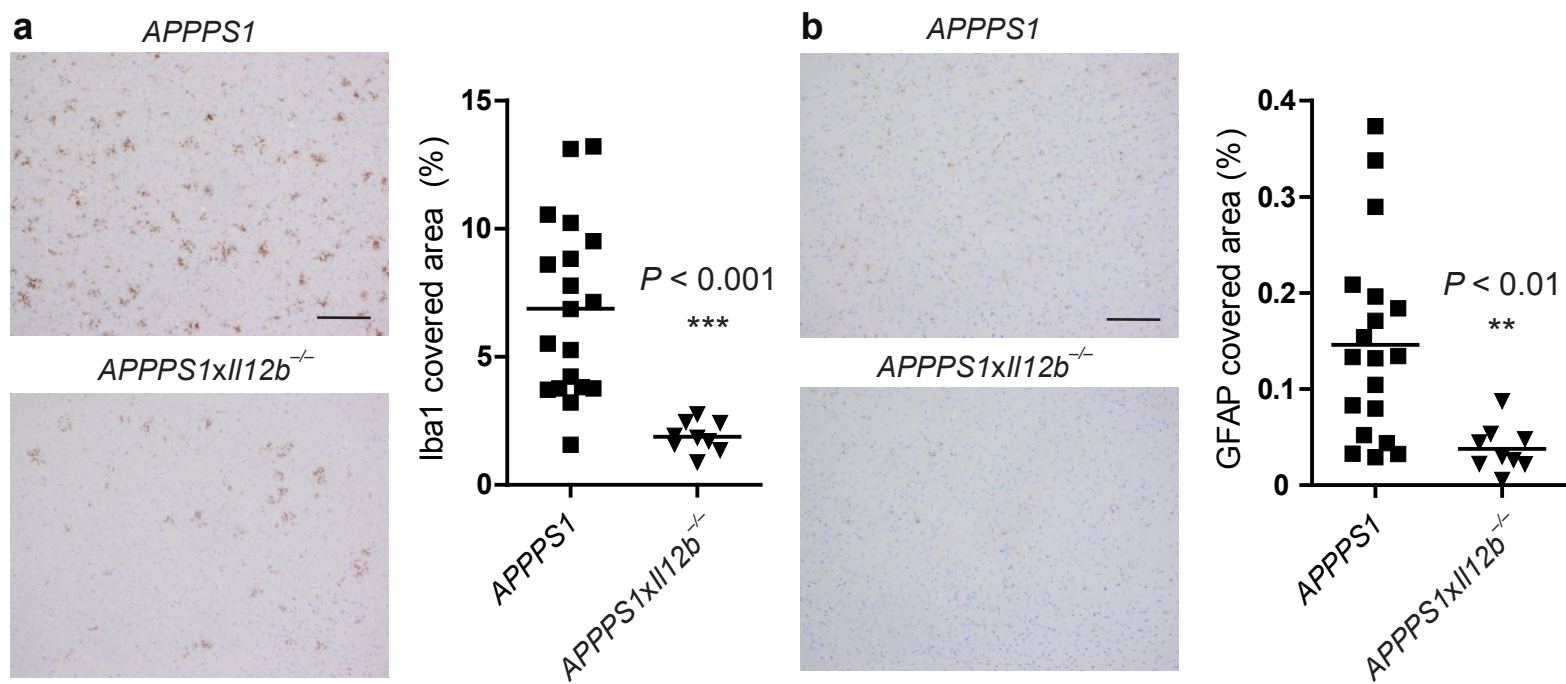
⁷These authors jointly directed the study

Corresponding authors

F.L.H. (frank.heppner@charite.de) or B.B. (becher@immunology.uzh.ch)

Supplementary Figure 1

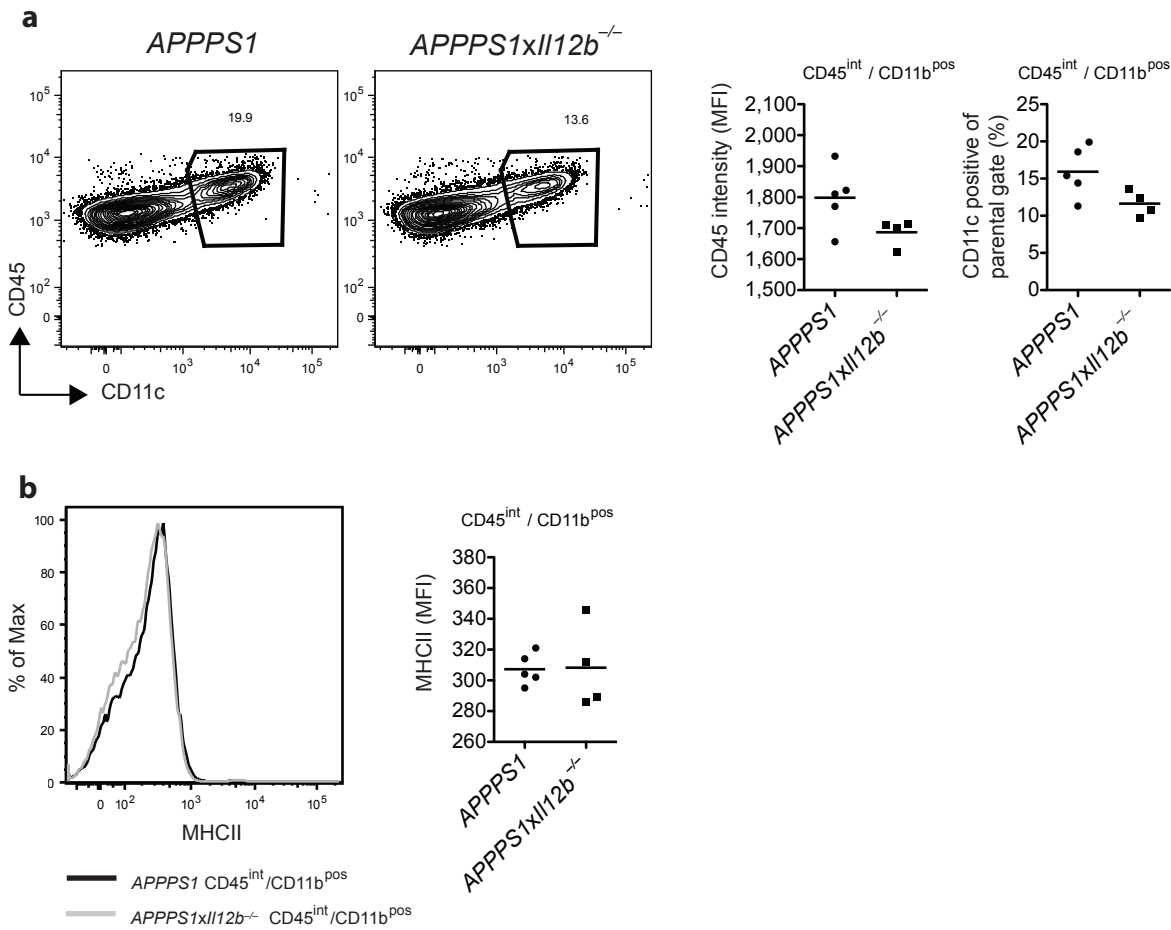
120 d



Supplementary Figure 1: Microglia/macrophages and astroglia in *APPPS1* and *APPPS1xII12b^{-/-}* mice at 120 d of age

Staining for and quantification of **(a)** microglia/macrophages (left: histological panel and morphometric quantification using Iba1 antibody, scale bar 100 μ m) and **(b)** astroglia (right: histological panel and morphometric quantification using GFAP antibody, scale bar 100 μ m) at 120 d of age in *APPPS1* ($n = 16$) and *APPPS1xII12b^{-/-}* ($n = 9$) animals. Each symbol represents the mean of the morphometrically assessed Iba1- or GFAP-covered area of one mouse.

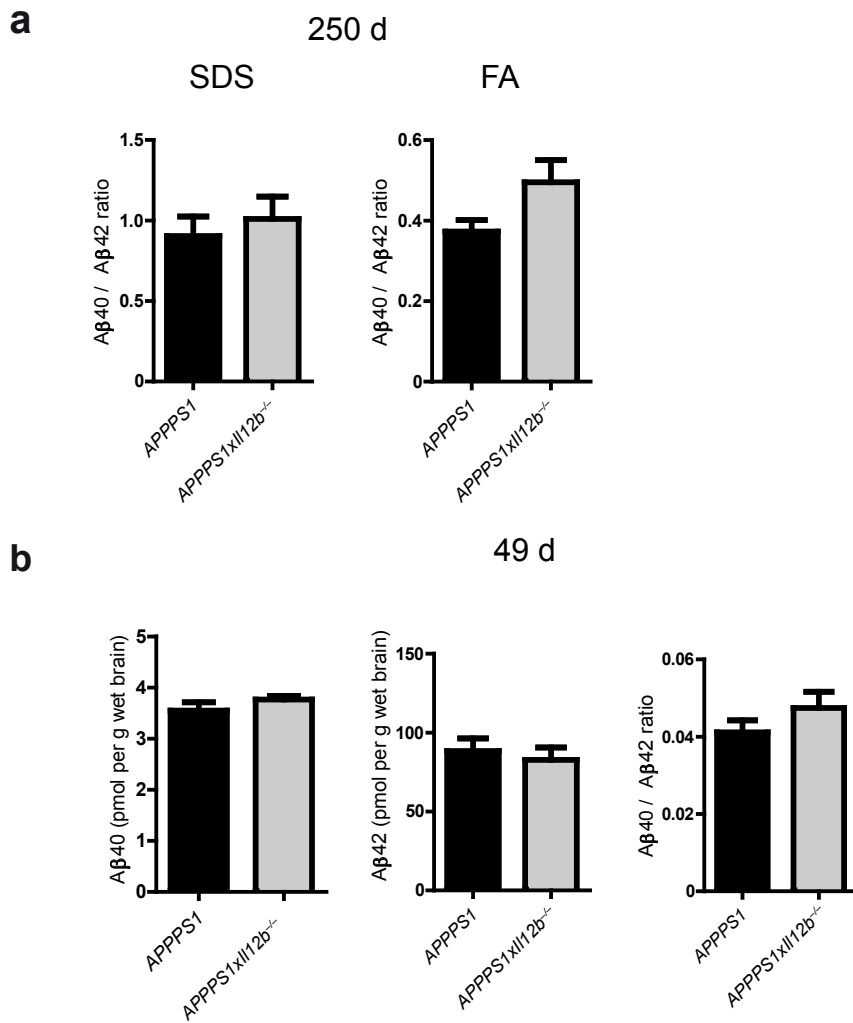
Supplementary Figure 2



Supplementary Figure 2: Microglial CD45 and CD11c expression in plaque-bearing *APPPS1xII12b^{-/-}* mice

Brain homogenates derived from 120 d old female *APPPS1* ($n = 5$) and *APPPS1xII12b^{-/-}* mice ($n = 4$) were stained for CD45, CD11b, CD11c and MHCII, analyzed by flow cytometry and gated on live singlet cells. **(a)** CD45^{int}/CD11b^{pos} cells were plotted for CD45 and CD11c expression; depicted gate illustrates CD11c positive cells, scatter plots on the right show the CD45 mean fluorescence intensity (MFI) and frequency of CD11c positive cells. **(b)** MHCII expression of CD45^{int}/CD11b^{pos} cells isolated from *APPPS1* (black line) or *APPPS1xII12b^{-/-}* (grey line) animals. Scatter plot on the right shows the MHCII MFI. Differences between the groups did not reach statistical significance.

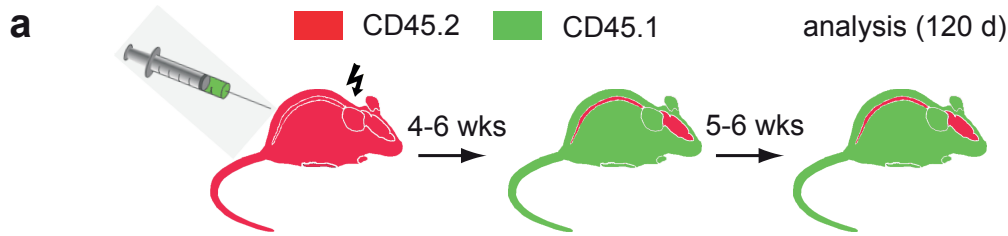
Supplementary Figure 3



Supplementary Figure 3: $A\beta_{40}/A\beta_{42}$ ratio in old, depositing (250 d) and young, pre-depositing (49 d) *APPPS1* and *APPPS1xIII12b*^{-/-} mice

(a) Calculation of the $A\beta_{40}/42$ ratio based on data retrieved by the Meso Scale enzyme linked immunosorbent assay (ELISA) method shown in Fig. 3a. Despite a trend towards an increased $A\beta_{40}/42$ ratio in the insoluble (FA) fraction, no significant difference in the $A\beta_{40}/42$ ratio between *APPPS1* and *APPPS1xIII12b*^{-/-} was detected. (b) Biochemical analysis was performed using homogenates of cerebral hemispheres of *APPPS1* and *APPPS1xIII12b*^{-/-} mice at 49 d of age ($n = 5-6$ per group). The amount of $A\beta_{40}$ and $A\beta_{42}$ protein in the SDS soluble fraction was assessed using a conventional ELISA. Again, no significant difference in the $A\beta_{40}/42$ ratio between *APPPS1* and *APPPS1xIII12b*^{-/-} mice was detected.

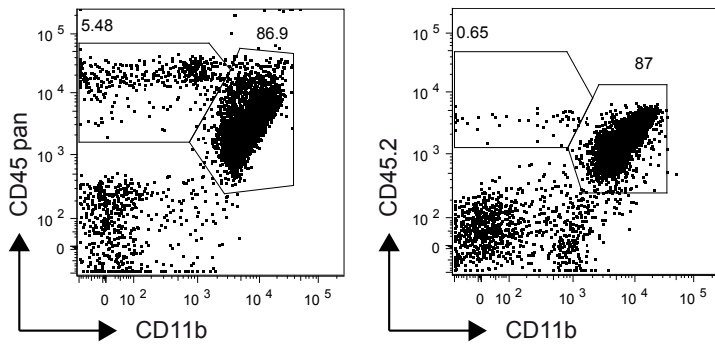
Supplementary Figure 4



b

Chimerism blood	Time after reconstitution	<i>Il12b</i> chimeric mice	<i>Il12rb1</i> chimeric mice
% CD45.1 pos	6 weeks	95.4±0.6	89.8±1.7
% CD45.1 pos	11 weeks	96.2±0.9	87.2±3.2

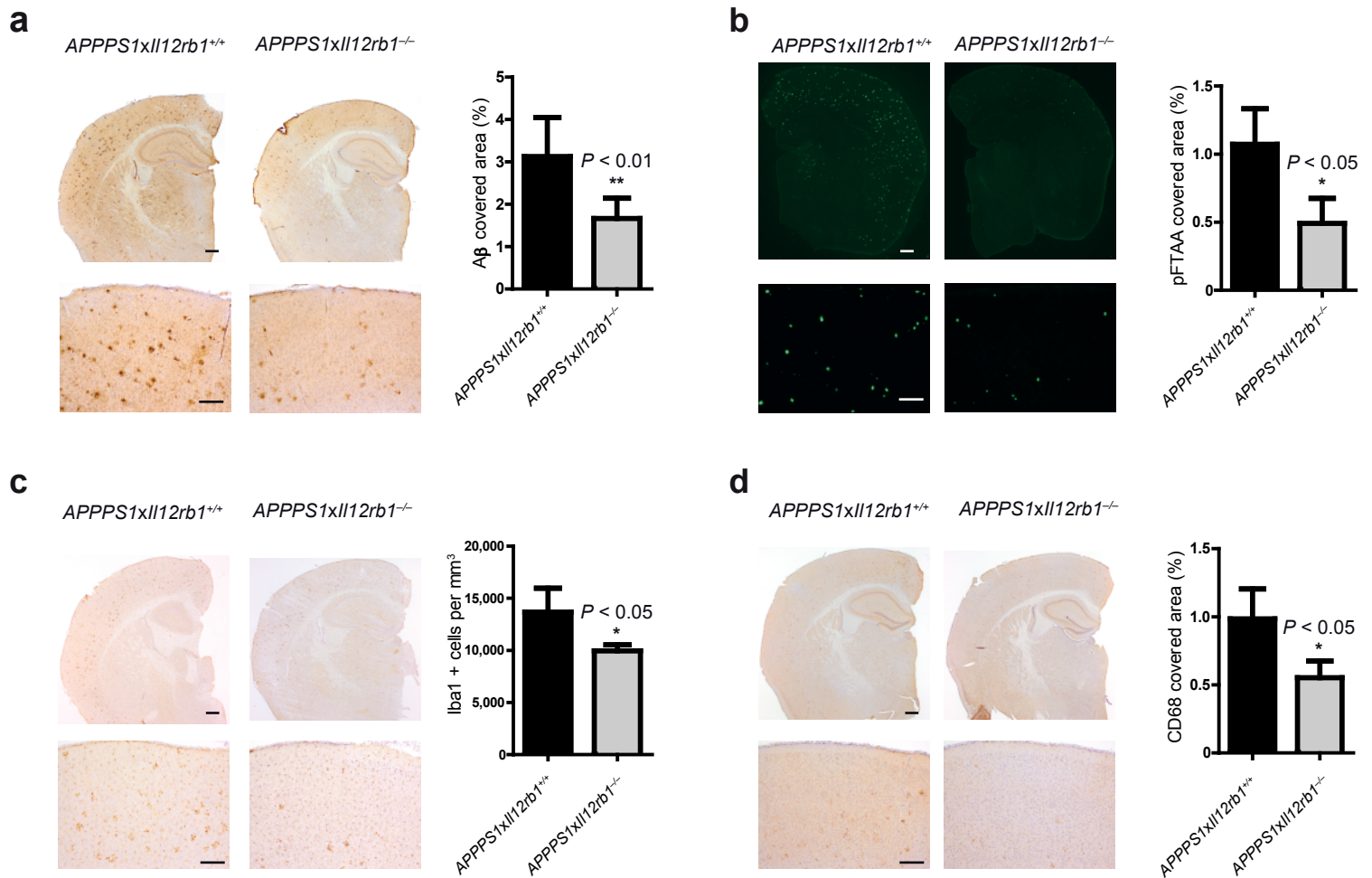
c Brain chimerism



Supplementary Figure 4: Analysis of chimerism in blood and brain

(a) Bone marrow recipients as depicted in **Fig. 4a** and **b** carry the congenic marker CD45.2 within the hematopoietic compartment, whereas bone marrow donors (WT, *Il12b*^{-/-} or *Il12rb1*^{-/-}) are CD45.1 positive. (b) Blood chimerism: flow cytometric analysis of blood for the congenic markers CD45 pan (recognizing both CD45.1 and CD45.2), CD45.1 and CD45.2 at 6 and 11 weeks after adoptive transfer of bone marrow and (the latter corresponding to the endpoint of the experiment). Time-point 6 weeks depicts the mean percentage and standard deviation of CD45.1 positive blood lymphocytes of individual mice; timepoint 11 weeks (120 d of age) displays the mean percentage and standard deviation of pooled blood samples from the experimental groups (see **Fig. 4a** and **b**). (c) Brain chimerism: representative dot plot of cells isolated from pooled cerebral hemispheres of *Il12b*^{-/-} → *APPPS1* × *Il12b*^{-/-} mice (similar results were obtained for the other experimental groups as depicted in **Fig. 4a** and **b**, data not shown). Cells were stained for CD45 pan, CD45.1, CD45.2 and CD11b. Dead cells and duplets were excluded. Left dot plot shows all CD45 positive cells (CD45 vs CD11b), right dot plot displays only the radio-resistant CD45.2 positive recipient-derived cells. Note that only lymphocytes (CD45^{hi}/CD11b^{neg}) are being replaced, while microglia (CD45^{int}/CD11b^{pos}) are not exchanged by this procedure.

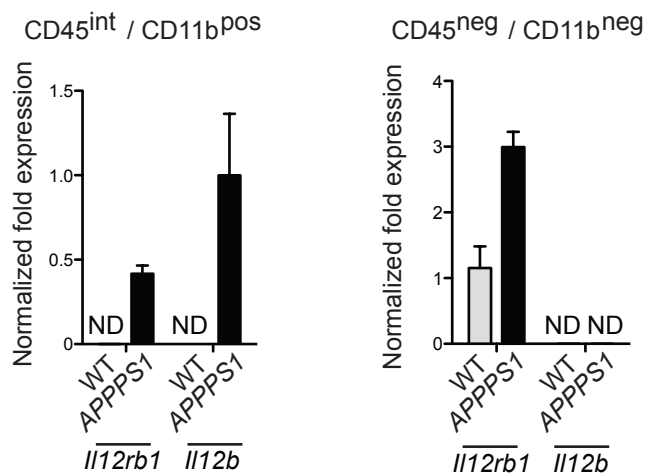
Supplementary Figure 5



Supplementary Figure 5: Genetic deletion of the IL-12 receptor-β1 subunit reduces plaque burden and microglial activation in *APP^{PS1}* mice

(a,b) Aβ burden in *Il12rb1*-deficient *APP^{PS1}* mice was assessed by immunohistochemical staining using the β-amyloid reactive antibody 4G8 (a) or pFTAA staining (b) (upper row: low magnification pictures, scale bar: 500 μm; lower row: higher magnification images, scale bar: 200 μm). Stereomorphometric analysis of β-amyloid covered area (right panel) in *APP^{PS1}* mice lacking the IL-12R-β1 subunit at 120 d of age, compared to control Alzheimer's *APP^{PS1}* mice with functional IL-12R-β1-mediated signaling. Aβ covered cortical area was stereomorphometrically assessed on 10 systematically randomly sampled 40 μm thick sections throughout the mouse cortex using the Microbrightfield® Stereoinvestigator system with the Cavalieri estimator. (c) Microglia number of the mice depicted in (a) was analyzed by immunohistochemical staining using the Iba1 antibody (upper row: low magnification pictures, scale bar 500 μm; lower row: higher magnification images, scale bar 200 μm). Number of Iba1 positive cells was stereomorphometrically assessed on 10 systematically randomly sampled 40 μm thick sections throughout the mouse cortex using the Microbrightfield® Stereoinvestigator system with the Optical fractionator method. (d) Microglia activation of the mice depicted in (a) was analyzed by immunohistochemical staining using the CD68 antibody (upper row: low magnification pictures, scale bar 500 μm; lower row: higher magnification images, scale bar 200 μm). Stereomorphometric analysis of CD68 covered area (right panel) was performed as described in (a). (a) $n = 6$ and (b-d) $n = 4$ mice were analyzed per group.

Supplementary Figure 6

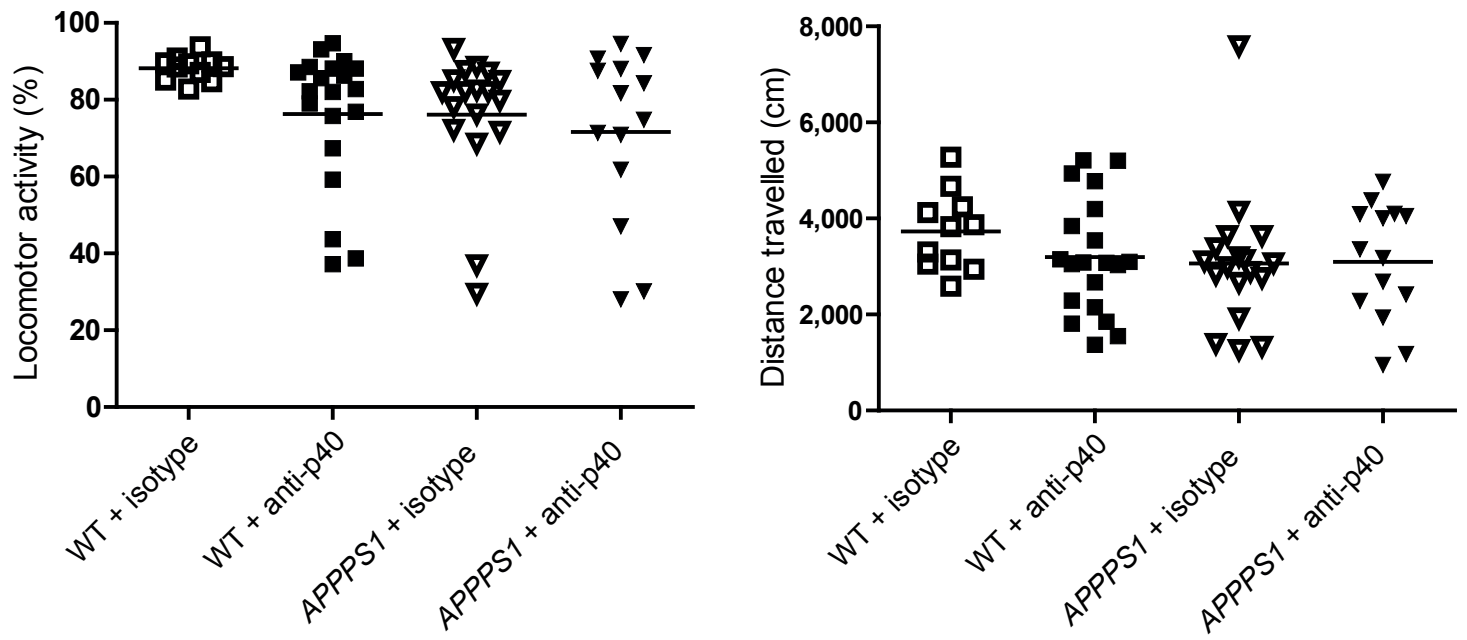


Supplementary Figure 6: Expression of *Il12rb1* in FACS sorted brain cells

200 d old male *APPPS1* ($n = 7$) and littermate control ($n = 4$) brain homogenates were stained for CD45 and CD11b and separated into the CD45^{int}/CD11b^{pos} microglia (left panel) and CD45^{neg}/CD11b^{neg} non-myeloid populations (right panel). Gene expression of *Il12rb1* and *Il12b* in FACS sorted populations was assessed in pooled samples. Depicted is the normalized fold change of expression in relation to Hypoxanthin-Guanin-Phosphoribosyltransferase (HPRT) levels. ND: not detectable; error bars depict s.e.m. of replicate wells.

Pooling of individual samples prior to the experiment precluded statistical analysis.

Supplementary Figure 7

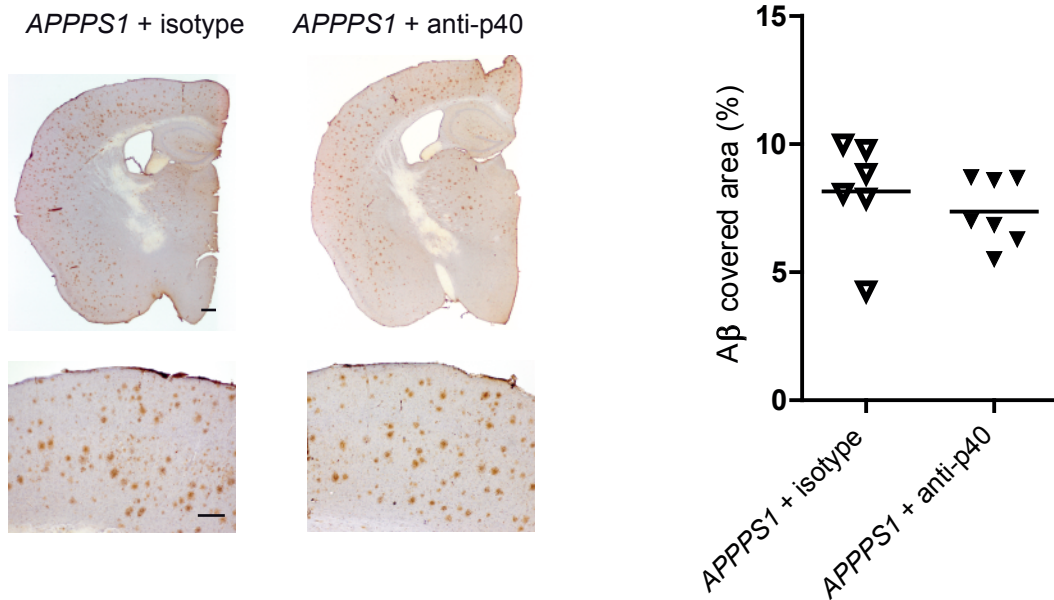


Supplementary Figure 7: Behavioral analysis of aged mice upon *icv* antibody delivery

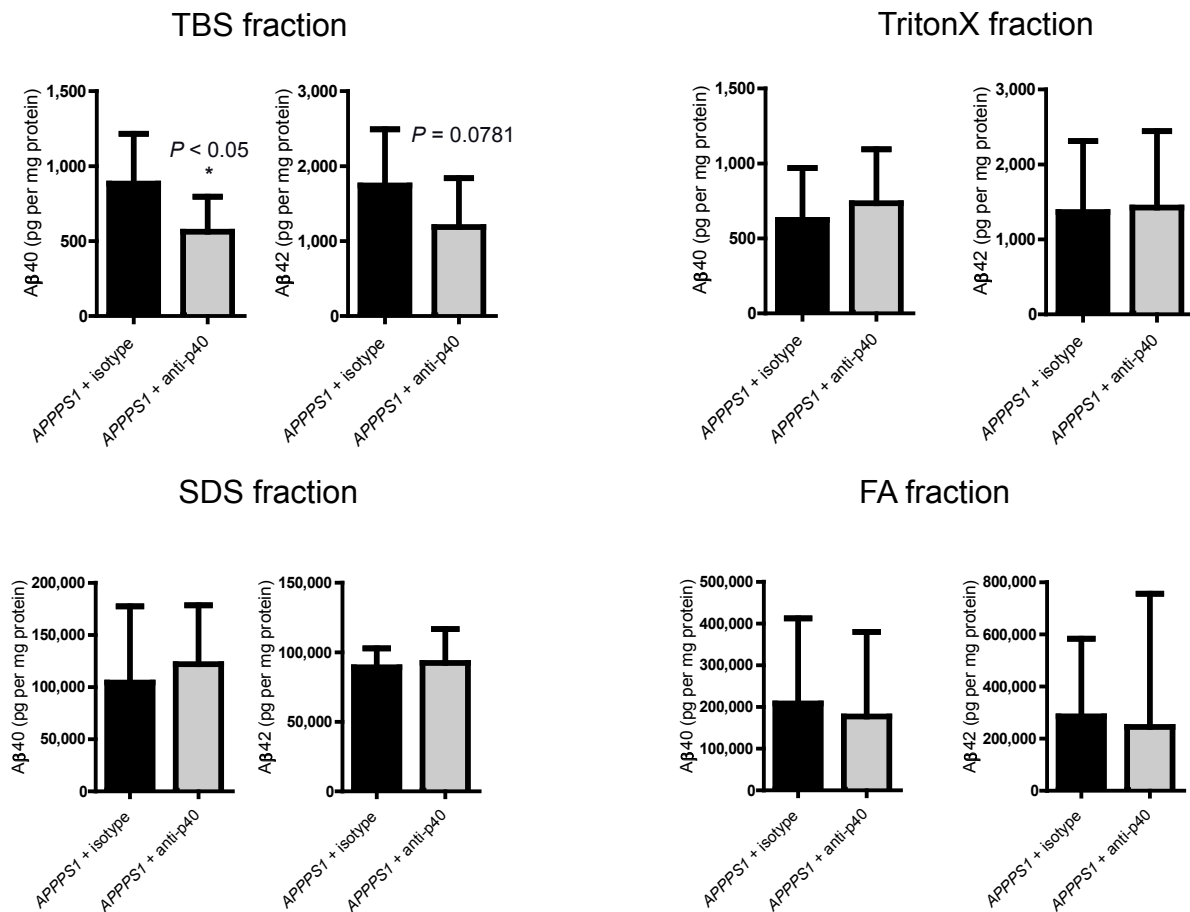
Aged WT and *APPPS1* mice (230 – 240 d of age) were subjected to behavioral analyses after 6 weeks of *icv* anti-p40 or isotype control antibody treatment as described in **Fig. 5**. Assessment of general locomotor activity in the Open-Field arena was quantified as locomotor activity (%) (left panel) and distance travelled (cm) (right panel). Hippocampus-dependent memory formation in mice described in **Fig. 5** was also measured in fear conditioning paradigm and revealed a trend towards reduced memory function in *APPPS1* mice, independent of treatment, which did not reach statistical significance (data not shown).

Supplementary Figure 8

a



b



Supplementary Figure 8 : Aβ burden and soluble Aβ levels in *icv* anti-p40 or isotype-control antibody treated *APPPS1* mice

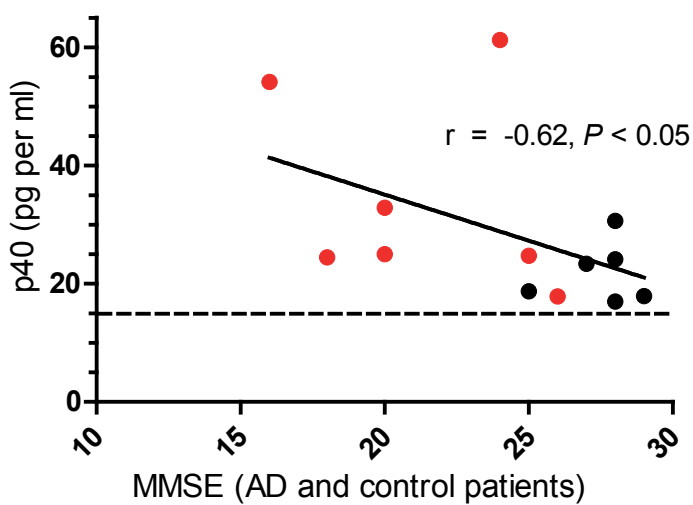
(a) Aβ burden in *APPPS1* mice treated with isotype control antibody ($n = 6$) or anti-p40 antibody ($n = 7$) *icv* (Fig. 5 and Supplementary Fig. 7) was assessed by immunohistochemical staining (left) and stereomorphometric analysis of the β-amyloid covered area (right) as described in Supplementary Fig. 5. (b) For analysis of soluble Aβ levels, snap frozen hemispheres of *APPPS1* mice treated *icv* with isotype control antibody ($n = 11$) or anti-p40 antibody ($n = 11$) as described in (a) were subjected to a 4-step extraction protocol⁴⁸. Protein amount of Aβ40 and Aβ42 in each fraction was quantified using the Meso Scale ELISA system as described for Fig. 3. Statistical analysis revealed no significant difference between those groups where no P value is indicated.

Supplementary Figure 9

a

group	sex	age (years)	MMSE score	A β 42 (pg per ml)	t-Tau (pg per ml)	p40 (pg per ml)
control	9m, 11f	68,80 (6,1)	28,15 (1,6)	1096 (374)	210 (68)	21,95 (5,17)
mild AD	9m, 11f	71,8 (7,5)	24,28 (2,8)	519 (156)	675 (308)	32,20 (19,65)
moderate AD	8m, 11f	72,21 (8,4)	16,11 (4,6)	474 (145)	697 (332)	37,14 (15,29)

b



Supplementary Figure 9: p40 protein values in CSF specimens of AD and control subjects

(a) Cohort details for the individuals included in the CSF analysis. Values are given as means with standard deviations in parentheses. p40 protein values represent the mean of samples above detection limit of the assay (15 pg per ml) within the given groups (control, $n = 6$; mild AD, $n = 4$; moderate AD, $n = 3$). (b) Correlation of MMSE and p40 protein values in AD and control patients. Dotted line indicates detection limit of ELISA system as described in (a). Each symbol represents p40 protein values of one patient (red dots represent data points from AD patients, black dots from control patients).